Dynamic Structure of a Highly Ordered β-Sheet Molten Globule: Multiple Conformations with a Stable Core†

Elisar Barbar,‡ George Barany,§ and Clare Woodward*,‡

Department of Biochemistry, University of Minnesota, St. Paul, Minnesota 55108, and Department of Chemistry, University of Minnesota, Minneapolis, Minnesota 55455

Received May 5, 1995; Revised Manuscript Received June 26, 1995⊗

ABSTRACT: The structure of $[14-38]_{Abu}$, a variant of bovine pancreatic trypsin inhibitor (BPTI) with only the 14−38 disulfide bridge intact, has been analyzed by two-dimensional ^1H and $^1H-^{15}N$ NMR. Except for the 18−24, 29−35 antiparallel β-sheet, residues in all regions of the molecule give two exchange cross peaks for each ^1H; for one residue, Gly 37, three exchange cross peaks are observed. The presence of exchange cross peaks indicates that the residues sample conformations that interconvert on a time scale of milliseconds or longer. Over 90% of the NMR spectra have been assigned, including backbone and side chain atoms and their exchange cross peaks. Analyses of chemical shifts, chemical exchange, hydrogen isotope exchange, and NOEs indicate that $[14-38]_{Abu}$ at pH 4.5 and 1 °C is an ensemble of interconverting conformations, in all of which the 18−24, 29−35 antiparallel β-sheet is native-like and intact. Outside the antiparallel β-sheet, residues undergo local order/disorder transitions. The stable structure of $[14-38]_{Abu}$ is not in the vicinity of the 14−38 disulfide bond but rather is in the slow-exchange core. NOE analysis indicates that the main tertiary interactions involve hydrophobic contacts with the rings of Tyr 21, Tyr 23, and Tyr 35. As a model for early folding intermediates, the structure of $[14-38]_{Abu}$ suggests that BPTI folding is initiated by stabilization of a turn existing in the unfolded protein and involves both local and nonlocal hydrophobic interactions.

BPTI[1] with only the 14−38 disulfide bridge intact has been chemically synthesized with the other four cysteines replaced by α-amino-*n*-butyric acid (Ferrer et al., 1992). At pH 4.5 and 1−10 °C, $[14-38]_{Abu}$ BPTI has the circular dichroism (CD) and fluorescent dye binding characteristics of a highly ordered molten globule, undergoes cooperative unfolding with a midpoint temperature of 19 °C, and regains >70% of its CD signal in ≤10 ms when folded from the acid-denatured state at pH 2.5 (Ferrer et al., 1995). Preliminary NMR analysis indicated that $[14-38]_{Abu}$ at pH 4.5 and 1 °C is partially folded. Here we report a full analysis of the dynamic structure of $[14-38]_{Abu}$ by homonuclear and heteronuclear NMR of site-specifically ^{15}N-labeled samples.

The structures of partially folded and molten globule species of proteins are of rising interest because it appears likely that they are models for transient intermediates formed during the protein folding process (Ptitsyn, 1992; Dobson, 1992; Baldwin, 1993; Redfield et al., 1994). Most molten globules for which detailed structural analyses are available are α-helical (Alexandrescu et al., 1993; Baum et al., 1989; Hughson et al., 1990; Jeng & Englander, 1991; Jennings & Wright, 1993). We have carried out a detailed structural analysis of a β-sheet molten globule, $[14-38]_{Abu}$, which gives insight into specifics of BPTI folding as well as generalizations of β-sheet folding. We find that $[14-38]_{Abu}$ is an ensemble of partially folded conformations interconverting on the millisecond or longer time scale. In all conformations, the antiparallel β-sheet is stable and native-like, while the rest of the molecule undergoes localized, segmental motions. NOE analysis indicates that both local and nonlocal hydrophobic tertiary interactions are critical to formation of partially folded $[14-38]_{Abu}$.

As a model for protein folding intermediates, the structure of $[14-38]_{Abu}$ is consistent with folding initiation by turns populated in unfolded species (Dyson & Wright, 1991), hydrophobic zippering (Dill et al., 1993), the view that denatured states are interconverting species with varying amounts of native structure (Dill & Shortle, 1991), and the slow-exchange core model for protein folding (Kim et al., 1993a). The stable, ordered structure is not in the vicinity of the 14−38 disulfide cross-link, and the primary effect of the disulfide appears to be destabilization of more unfolded forms due to loss of chain entropy. Comparison of NMR-detected structures of $[14-38]_{Abu}$ and of reduced BPTI (Kemmink & Creighton, 1993; Pan et al., 1995) points to specific interactions in the unfolded state that may favor nucleation of the antiparallel β-sheet in early folding steps. Implications for disulfide-linked folding of BPTI are that formation of any single, native-like disulfide bond stabilizes the slow-exchange core and, depending on the disulfide, stabilizes one or both helices by destabilizing their more disordered conformations.

MATERIALS AND METHODS

Sample Preparation. $[14-38]_{Abu}$ was prepared by automated Fmoc solid-phase synthesis and purified essentially

† This work was supported by NIH Grants GM 26242 (C.W.) and GM 51628 (G.B. and C.W.).

* Author to whom correspondence should be addressed.

‡ University of Minnesota, St. Paul.

§ University of Minnesota, Minneapolis.

⊗ Abstract published in *Advance ACS Abstracts,* August 1, 1995.

[1] Abbreviations: Abu, α-amino-*n*-butyric acid; BPTI, bovine pancreatic trypsin inhibitor; NMR, nuclear magnetic resonance; HPLC, high-performance liquid chromatography; NOESY, nuclear Overhauser effect spectroscopy; ROESY, rotating frame Overhauser effect spectroscopy; TOCSY, total correlation spectroscopy; HMQC, heteronuclear multiple quantum coherence; HSQC, heteronuclear single quantum coherence; TSP, 3-(trimethylsilyl)[$^2H_4$]propionate.

0006-2960/95/0434-11423$09.00/0

as described elsewhere (Ferrer e al., 1992); methodological refinements gave materials with improved purities of >98%. For heteronuclear NMR experiments, ^{15}N-labeled amino acids were incorporated into selected positions in $[14-38]_{Abu}$ during synthesis. Purity was determined by analytical HPLC C-4 reversed-phase chromatography and capillary zone electrophoresis. Amino acid analyses and ion electrospray mass spectrometry of the purified proteins were in good agreement with the theoretical values. For $[^{15}N][14-38]_{Abu}$, mass calculated is 6451.6, and mass found is 6450.4 ± 1.4. The lyophilized pure product was dissolved at pH 2−4 and then dialyzed against water at pH 4.5. All pH values reported are the uncorrected glass electrode readings adjusted with dilute NaOH/HCl solutions. Like many partially folded states, $[14-38]_{Abu}$ has limited solubility, which requires use of fairly dilute solutions. NMR spectra reported here were obtained at pH 4.5−4.6, 1−10 °C, and a protein concentration of 0.5 mM. This concentration was chosen from extensive UV and circular dichroism solubility experiments with $[14-38]_{Abu}$ (Ferrer et al., 1995). To rule out the likelihood of aggregation effects, spectra were also obtained for samples diluted 10-fold; no changes in line widths, chemical shifts, or NOEs were detected.

NMR Spectroscopy. NMR spectra were obtained on Bruker AMX-500 and -600 spectrometers. The data were acquired with a spectral windows of 8.5 and 7 kHz on the AMX-600 and -500 instruments, respectively. The residual solvent line was presaturated using low power during the 1 s relaxation delay. Typically 300−400 t_1 values were obtained, and free induction decays for t_2 were recorded in 2048-point blocks, summing at least 128−256 acquisitions each. TPPI was used for phase-sensitive detection in t_1 in all two-dimensional spectra (Marion & Wüthrich, 1983). NOESY (mixing time, t_m, of 100 or 150 ms) (Jeener et al., 1979), clean TOCSY (Griesinger et al., 1988) (t_m of 30−85 ms, and spin-lock power of 11 kHz), and ROESY (t_m of 40, 50, or 100 ms) (Bothner-By et al., 1984; Bax & Davis, 1985) spectra were collected. Proton chemical shifts were measured from internal TSP standard at 0 ppm or water resonance at 4.99 ppm. For solvent suppression, NOESY spectra were acquired with a jump−return sequence (Hore, 1983) with a delay of 160 μs and a mixing time of 100−150 ms. NOESY spectra were also acquired with a pulse field gradient for water suppression using a 3−9−19 pulse sequence (Piotto et al., 1992) with a delay of 116 μs and a mixing time of 160 ms. Assignments or NOEs were determined from TOCSY and NOESY spectra obtained at different temperatures in the range 1−10 °C, with different mixing times, and in ^1H_2O as well as ^2H_2O. NMR data were processed and analyzed on a Silicon Graphics workstation using the program FELIX 2.3 (Biosym) or Bruker UXNMR. Data points were weighted by a squared sine bell in each dimension and zero filled to form 2K × 2K real matrices.

A number of experiments were carried out to investigate the conformational changes evident as exchange peaks in the amide region of the ^{1}H 2D TOCSY and NOESY. These included a series of TOCSY spectra recorded at increasing temperatures and different mixing times. TOCSY and ROESY spectra with different spin-lock mixing times and low spin-lock power contain cross peaks due to slow exchange between conformations. A weak spin-lock field with a 90° pulse of 34 μs was used.

For heteronuclear assignments, HSQC experiments (Bodenhausen & Ruben, 1980), 2D HMQC-NOESY (t_m of 175 ms), and 2D HMQC-TOCSY (t_m of 70 ms) (Bax et al., 1983) were obtained on the AMX-600 with a ^{15}N frequency of 60.82 MHz. ^{15}N decoupling during acquisition employed the WALTZ-16 sequence (Shaka et al., 1983). Spectra were acquired at 1 °C using spectral widths of 7.2 kHz in the ^{1}H dimension and 3.6 kHz in the ^{15}N dimension. Relative populations of conformations in slow chemical exchange were estimated by measuring peak intensities in ^{15}N HSQC spectra acquired with preirradiation of the water resonance for 3 μs and a long relaxation delay of 3 s. The residual water resonance was suppressed by a high-power ^{1}H spin-lock purge pulse applied for 0.7 ms (Messerle et al., 1989).

Hydrogen isotope exchange rates were obtained by measuring peak intensities vs time in a series of 1D spectra at pH 4.5 and 1 °C. Pseudo-first-order rate constants were determined from nonlinear least-squares fit of an exponential rate equation to experimental data.

RESULTS

Assignments. NMR spectra were obtained at pH 4.6 and 1−10 °C, conditions where $[14-38]_{Abu}$ forms a highly ordered β-sheet molten globule (Ferrer et al., 1995). Compared to equivalent spectra of native BPTI (Wagner et al., 1987), those of $[14-38]_{Abu}$ contain additional cross peaks with chemical shifts commonly observed in disordered peptides. For example, the NOESY spectrum in Figure 1 has more NH cross peaks than native BPTI between 8.2 and 8.8 ppm, the region for NH chemical shifts in unfolded proteins. Similar clustering in the random coil region is found in TOCSY spectra (Figure 2). However, both NOESY and TOCSY spectra of $[14-38]_{Abu}$ also have numerous cross peaks well removed from the random coil envelope. For the resolved cross peaks, assignments were made from combined analysis of TOCSY spin systems and NOESY primary and secondary structural connectivites, long-range NOEs, and amide hydrogen exchange rates. For example, NOESY connectivities of β-sheet strands 18−24 and 29−35 are shown in Figure 3. Having assigned the well-resolved cross peaks, we then found that many are in slow chemical exchange with NH resonances clustered within the random coil region, and this enabled us to assign most of the clustered resonances.

Slow chemical exchange arises when the same proton has a different chemical shift in each of two or more conformations that interconvert on the time scale of milliseconds or longer, thereby giving rise to a distinct signal for each conformation (Sandström, 1982). NH−NH cross peaks observed in the low-field region of TOCSY, NOESY, and ROESY spectra arise from conformational exchange that is fast on the NMR T_1 scale but slow on the chemical shift time scale. Figure 4a shows the downfield region of a TOCSY spectrum of $[14-38]_{Abu}$ containing NH cross peaks due to slow chemical exchange between different conformations. In comparison, an equivalent native BPTI spectrum shows no cross peaks (Figure 4b), because only the average native conformation is reported by each NH. The exchange cross peaks were assigned by correlation to previously assigned cross peaks (as described above) and verified by identification of their respective spin systems in full TOCSY spectra. The assignments were confirmed further by ROESY

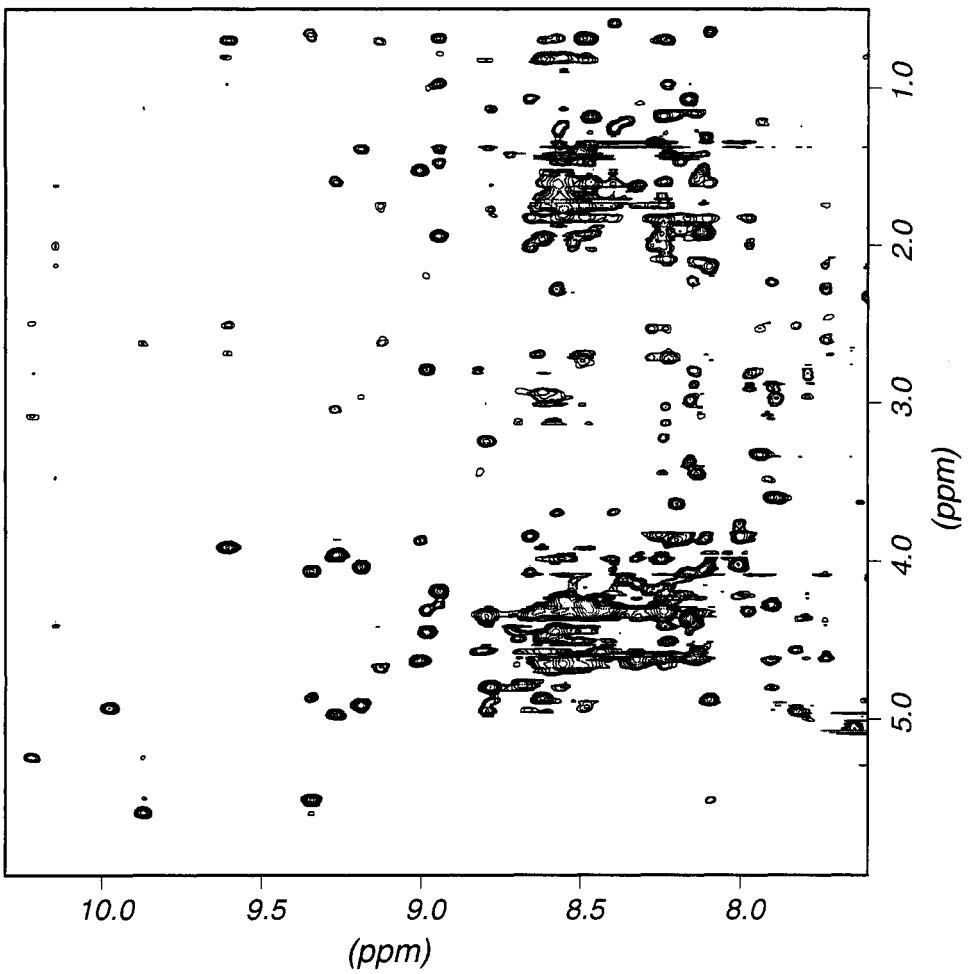

FIGURE 1: 500-MHz NOESY spectrum of $[14-38]_{Abu}$. The spectrum was recorded at 1 °C and pH 4.6 in 90% ^1H_2O/10% ^2H_2O. Overlapping peaks between 8.2 and 8.8 ppm are due primarily to a disordered conformation in chemical exchange with a more ordered conformation. Chemical shifts of the latter are for the most part outside the 8.2−8.8 ppm region.

spectra, which have cross peaks of the same sign as the diagonal peaks (Bax & Davis, 1985) (data not shown), and by analysis of $^{15}N-^1H$ HMQC-TOCSY and -NOESY spectra (below). Collectively, the spectral correlations used to assign exchange cross peaks indicate that they are neither artifacts nor impurities. Slow conformational exchange detected by NMR has been reported between conformations of native interleukin-1β (Driscoll et al., 1990) and BPTI (Otting et al., 1993) and between folded and unfolded conformations of the N-terminal SH3 domain of drk (Zhang et al., 1994) and of 434 repressor (Neri et al., 1992).

Resonance assignments were made for more than 90% of $[14-38]_{Abu}$ TOCSY and NOESY spectra (assignments are available as supporting information). For exchange cross peaks of the same hydrogen, assignments are designated (f), (u′), or (u). Those with chemical shifts outside the random coil envelope are assigned to a more folded (f) conformer and often show NOEs indicating stable structure. Cross peaks with chemical shifts near, but not in, the random coil envelope and with no medium- or long-range NOEs are assigned to an unfolded, but not fully disordered (u′), conformer; their chemical shifts are different from random coil by ≥0.3 ppm. Cross peaks having chemical shifts within 0.3 ppm of equivalent hydrogens in random coils, and with no medium- or long-range NOEs, are assigned to a fully disordered (u) conformation. Random coil chemical shifts of NHs are taken as those observed in tetrapeptides at pH 7 and 35 °C (Wüthrich, 1986).

Site-specific, ^{15}N-labeled samples were used to verify assignments and exchange cross peaks. Eight ^{15}N-labeled amino acids were incorporated selectively into $[14-38]_{Abu}$: L6, G12, A16, L29, G37, A40, A48, and G56. Spin systems were assigned in $^{15}N-^1H$ HMQC-TOCSY spectra (Figure 5a). The presence of more than eight cross peaks reflects multiple conformations; in $^{15}N-^1H$ HMQC-NOESY spectra (Figure 5b), one NH gives rise to multiple peaks. Figure 5b contains three types of cross peak: those arising from $^{15}N^1H-^{14}N^1H$ NOEs, exchange peaks of the same $^{15}N^1H$ (auto peaks), and cross-correlation peaks of the auto peaks (unlabeled peaks at the vertices of dashed lines). NOE cross peaks labeled in Figure 5b are 6 NH (7.51 ppm) to 7 NH (7.74 ppm) and 5 NH (7.40 ppm), 11 NH (9.20 ppm) to 12 NH (7.35 ppm), 28 NH (8.18 ppm) to 29 NH (6.76 ppm), 39 NH (9.29 ppm) to 40 NH (7.50 ppm), 40 NH to 35 ring proton (6.90 ppm), 38 NH (8.01 ppm) to 37 NH (7.47 ppm), and 49 NH (8.67 ppm) to 48 NH (8.09 ppm). The other cross peaks observed are auto peaks and their cross-correlation peaks. For example, there are two auto peaks for 40 NH, one for a more folded (f) conformation (7.50/117.9 ppm) and a second for a more disordered or unfolded (u) conformation (8.5/125 ppm). The dashed lines connecting the 40 NH auto peaks intersect at their cross-correlation

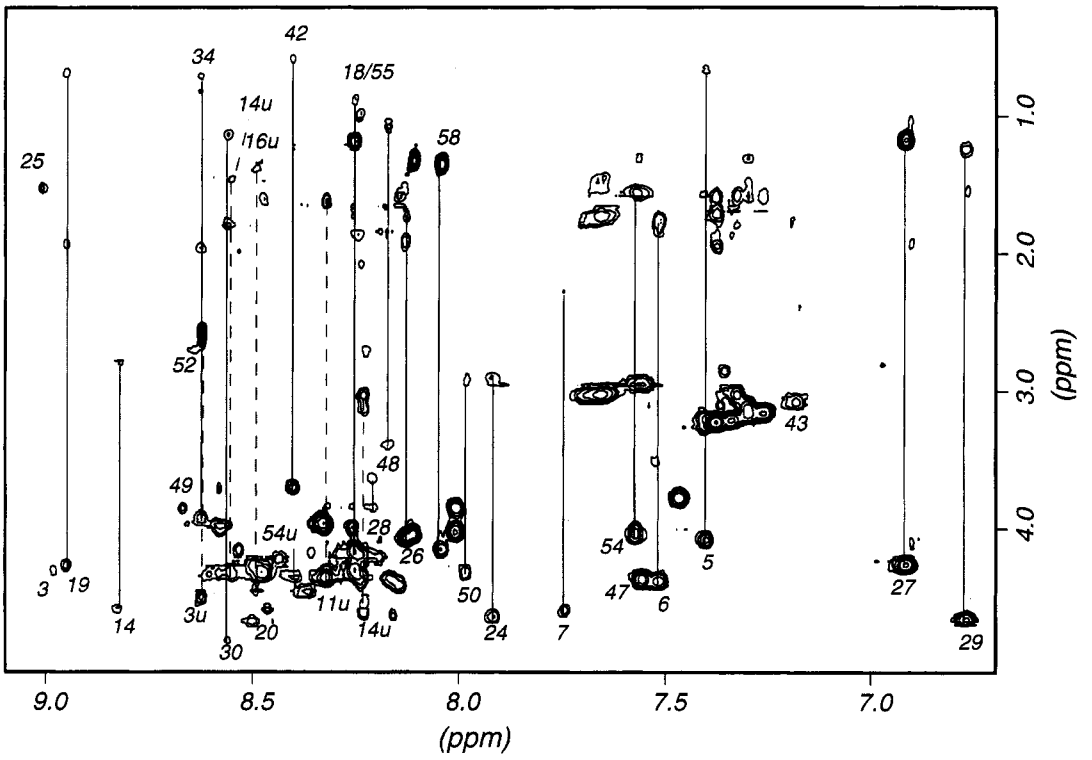

FIGURE 2: 600-MHz TOCSY spectrum of $[14-38]_{Abu}$ showing some assignments. The spectrum was recorded at 1 °C and pH 4.6 with a mixing time of 60 ms. Assignments are shown by vertical lines that connect cross peaks within the same spin system. The dashed lines are for the amino acids of the disordered population, labeled (u).

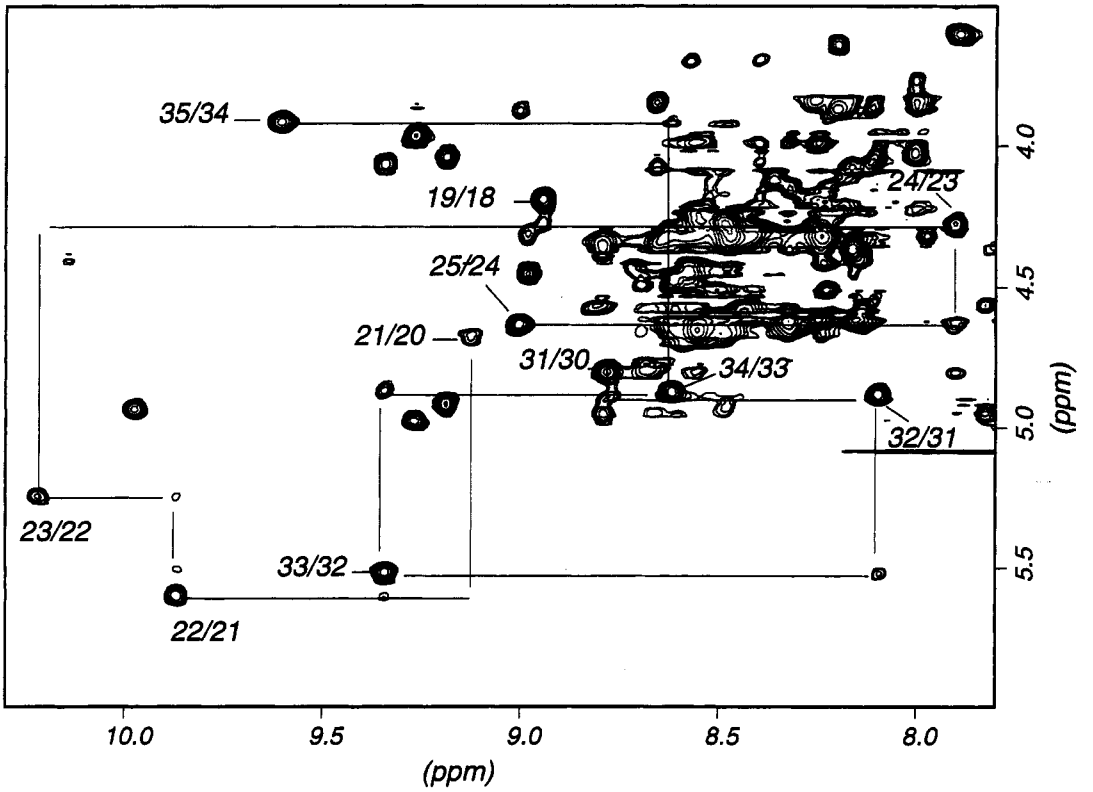

FIGURE 3: Fingerprint region of a NOESY spectrum showing NH to CαH sequential connectivities. The spectrum was acquired with a jump–return sequence for solvent suppression and a mixing time of 150 ms. Lines connect sequential NOEs for residues 18–25 and 30–35. Numbers label NOE cross peaks between sequential NH and CαH. The same connectivities were observed at a mixing time of 100 ms.

peaks (7.50/125 ppm and 8.5/117.9 ppm). Similar auto and correlation peaks are observed for 6, 29, and 37, and 48 NHs (not all are shown in Figure 5b). The observation of cross correlation peaks depends on the mixing time during which exchange is allowed to develop. Recent papers by Kay and associates (Farrow et al., 1994, 1995), in which global

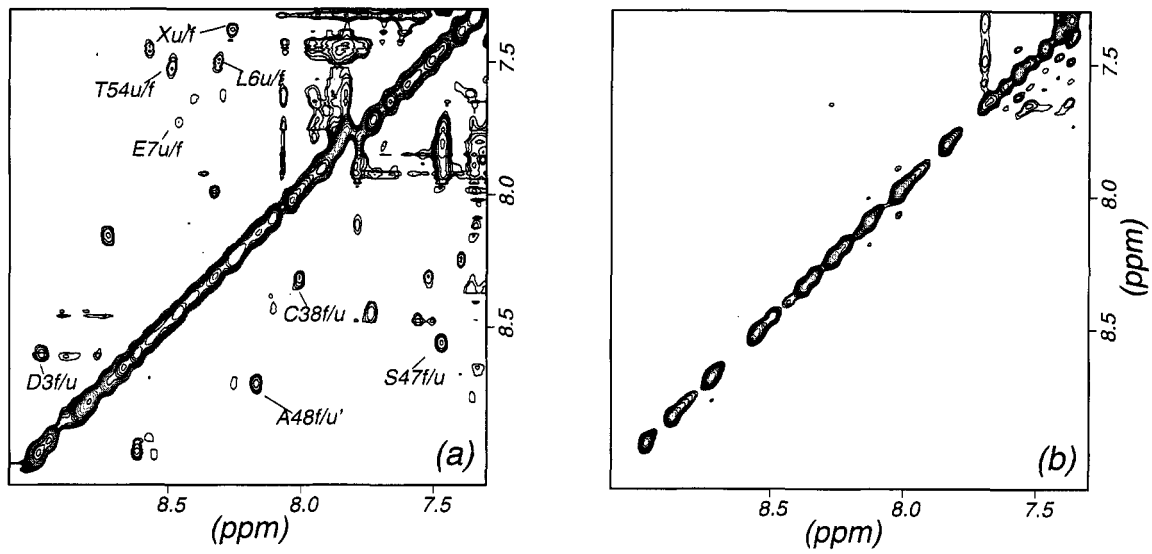

FIGURE 4: (a) TOCSY spectrum of $[14-38]_{Abu}$ showing cross peaks due to slow chemical exchange of amide hydrogens between more folded (f) and more disordered (u) conformations. All cross peaks are assigned, and some are labeled. Exchange cross peaks of amide hydrogens are also observed in ROESY and NOESY spectra. (b) Equivalent TOCSY spectrum of native BPTI showing no exchange cross peaks. Spectra were acquired in 90% ^1H_2O/10% ^2H_2O with a 60 ms mixing time and a low spin-lock power.

unfolding rather than segmental motions were measured, show that the interconversion rates can be estimated from volume intensities of cross-correlation peaks by varying the mixing times.

Relative populations of (f):(u) or (f):(u′) are determined for a few residues for which exchange cross peak volumes were estimated: Leu 6, 40:60; Leu 29, 85:15; Ala 40, 50:50; Ala 48, 60:40. Further analyses of spectra of $[14-38]_{Abu}$ are being carried out to determine equilibrium populations and interconversion rates of the conformational exchange reaction for each NH (E. Barbar, G. Barany, and C. Woodward, unpublished results). Although most residues for which exchange cross peaks are identified indicate slow interconversion between two conformations, one residue, Gly 37, has three exchange peaks (Figure 6), showing that this residue samples three slowly interconverting conformations.

NOEs. Short-range sequential and medium-range NOEs of $[14-38]_{Abu}$ indicative of secondary structure are summarized in Figure 7 for the most folded (f) conformation. Strong $d_{\alpha N}(i, i+1)$ NOEs for residues 18−36 are indicative of extended β-sheet strands. Strong $d_{NN}(i, i+1)$ NOEs in addition to medium-range $d_{\alpha N}(i, i+3,4)$ and $d_{\alpha\beta}(i, i+3,4)$ NOEs usually indicate an α-helical structure (Wüthrich, 1986). This pattern is observed only for residues 48−51, which form the first turn of the C-terminal helix in the native protein. Long-range backbone NOEs indicative of antiparallel β-sheet structure are listed in Table 1; 18−24 and 29−35 show long-range NH(i)−CαH(j) and NH(i)−NH(j) NOEs where residues i and j face each other, as well as CαH(i)−CαH(j) NOEs. A number of long-range NOEs, reflecting stable tertiary structure in $[14-38]_{Abu}$, were also observed (Table 2). All NOEs observed are listed in Tables 1 and 2 and Figure 7.

Hydrogen Isotope Exchange. Hydrogen isotope exchange rates were determined for slowly exchanging peptide NHs at pH 4.6 and 1 °C. Rate constants were obtained from 1D rather than 2D spectra because of limited solubility and fast exchange. Circles in Figure 7 mark residues with slow, medium, and fast NH exchange; those without circles exchange too rapidly to be measured by this method. Table

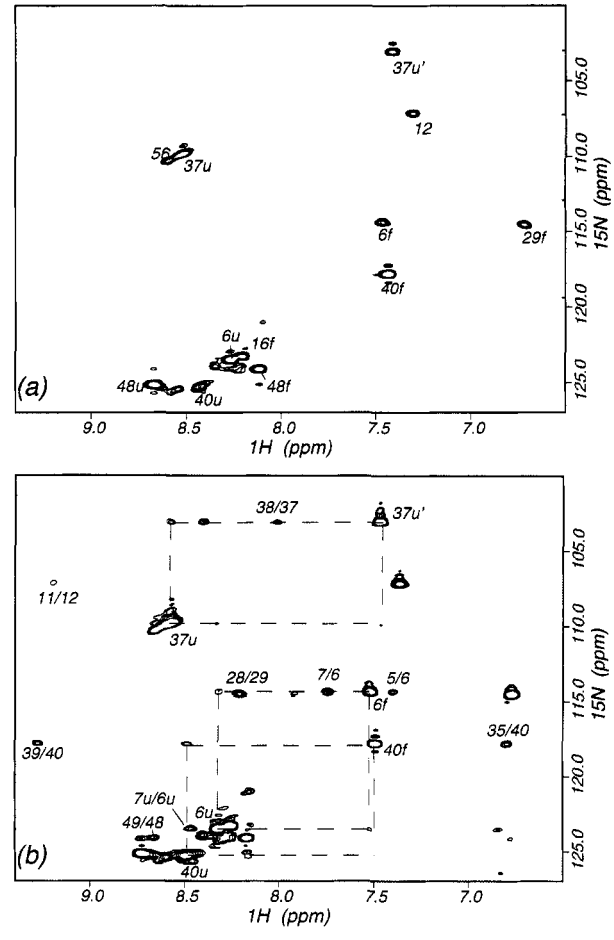

FIGURE 5: (a) $^{15}N-^1H$ HMQC-TOCSY and (b) HMQC-NOESY spectra of specifically labeled $[^{15}N][14-38]_{Abu}$. Cross peaks are labeled in (a) according to their amino acid sequence number. In (b), auto and exchange cross peaks of some residues are connected by dashed lines. The designators f and u in peak labels are explained in the text. Cross peaks labeled with two numbers are due to NH−NH sequential NOEs, except 35/40 which is an NOE between the 35 CεH at 6.80 ppm and the 40 NH at 7.48 ppm. Peaks labeled with one number are auto peaks. Dashed lines connect auto peaks and cross-correlation peaks as described in the text.

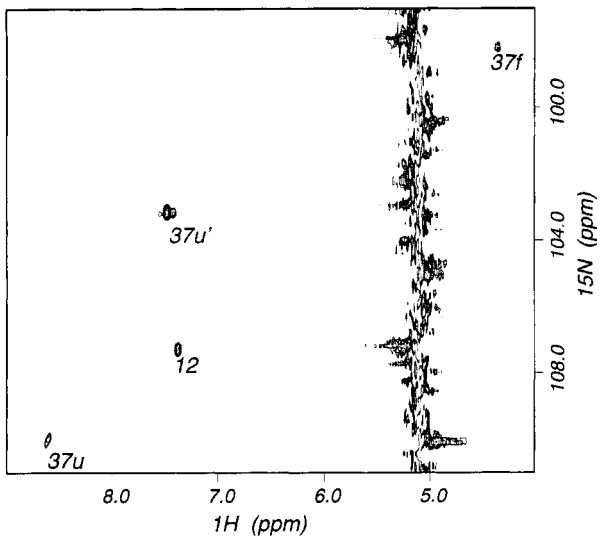

FIGURE 6: $^{15}N-^{1}H$ HSQC spectrum showing the three conformations of G37. The spectrum was acquired with a 3 s relaxation delay, using purge pulses for further suppression of the water (Messerle et al., 1989).

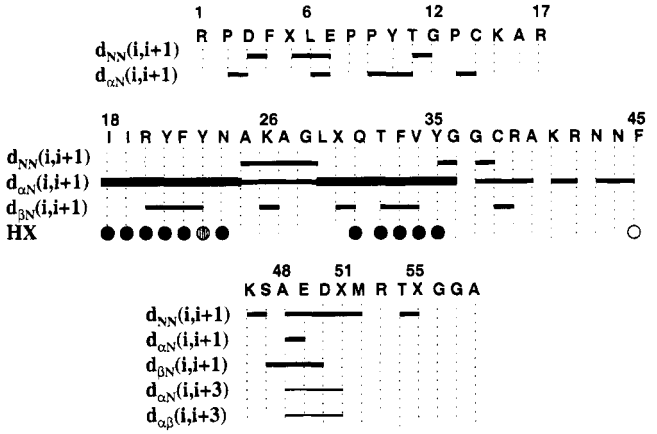

FIGURE 7: Summary of sequential assignments for $[14-38]_{Abu}$ at 1 °C, pH 4.5, for the (f) conformation. The bars below the sequence indicate the observed NOE connectivities. Thicker bars show greater intensities. The strong αN(i, i + 1) NOEs, in the absence of NN(i, i + 1), are indicative of β-sheet conformation. The medium-range αN(i, i + 3) and αβ(i, i + 3) between residues 48 and 51 are indicative of the presence of the first turn of the C-terminal helix. In the bottom row, filled circles mark the amide peaks that exchange the slowest, whereas hatched and open circles indicate medium and fast exchange rates, respectively. The rest of the amide protons rates could not be measured either because the exchange was too fast or because of overlapping protons. In either case, they exchange much faster than NHs of the core residues.

3 gives exchange rate constants and protection factors. Exchange rates for 18, 20, and 24 NH could only be estimated, due to resonance overlap. The slowly exchanging NHs in $[14-38]_{Abu}$ have rate constants that are smaller by factors of 10−40 than those in equivalent small peptides (Bai et al., 1993). Protection factors are different for every proton, except 21 and 22 NH, indicating that most exchange involves fluctuations of the partially folded state rather than global unfolding (Woodward, 1993). Tyr 21 and Phe 22 NHs have the slowest exchange rates and similar protection factors (Table 3); therefore, they may exchange by an unfolding mechanism. In native BPTI, Tyr 21, Phe 22, and Tyr 23 NHs are the slowest to exchange: 21 and 22 NHs are H-bonded to backbone oxygens in the middle of the

Table 1: Long-Range NOEs Showing Stable β-Sheet in $[14-38]_{Abu}$

residue	CαH NOEs[a]		NH NOEs[a]	
Ile 18			NH	Y35 NH
Ile 19	CαH	V34 CαH		
Tyr 21	CαH	T32 CαH; CβH		
Phe 22	CαH	R20 CβH	NH	X30 CγH
			NH	Q31 NH
			NH	F33 CεH
Tyr 23	CαH	X30 CαH	NH	L29 CδH
Phe 33			NH	R20 NH
Phe 45			NH	Y21 NH
			NH	R20 CβH

[a] NOEs were obtained from $^{1}H-^{1}H$ and $^{1}H-^{15}N$ NOESY spectra in $^{1}H_2O$ and $^{2}H_2O$. Abu is designated X.

Table 2: Long-Range NOEs Showing Tertiary Interactions in $[14-38]_{Abu}$

residue	long-range NOEs[a]	
Arg 20	NH	I19 CδH1 (w)
	CβH	F45 CδH (w)
Tyr 21	NH	K46 CβH (w)
	CαH	T32 CγH (w)
	CδH	A48 CαH (w); CβH (m)
	CδH	K46 CαH (w); CβH (w); CγH (w)
	CδH	T32 CγH (m)
	CδH	X30 CγH (m)
	CδH	R20 CαH (w)
	CεH	A48 CβH (m)
	CεH	K46 CαH (w)
	CεH	T32 CγH(m); CβH (w)
Phe 22	CαH	F45 CδH (w)
	CδH	N24 CαH (m)
	CεH	N24 CαH (w); CβH1 (w); CβH2 (w)
	CζH	N24 CαH (m); CβH1 (w); CβH2 (m)
Tyr 23	NH	N43 NδH1; NδH2 (w)
	CδH	A25 CαH (m); CβH (m)
	CδH	X30 CαH (w); CβH1; CβH2 (m)
	CεH	A25 CαH (m); CβH (m)
	CεH	L29 CαH (w); CβH (w)
Abu 30	CδH	A48 CαH (w)
Tyr 35	CδH1	I18 CγCH$_3$ (m); CδH (m)
	CεH1	I18 CγCH$_3$ (m); CδH (m)
	CδH2	T11 CαH (w)
	CδH2	A40 CαH (w); CβH (w)
	CδH2	G37 NH (w)
	CεH2	A40 NH (m),CαH (m); CβH (m)
Gly 36	NH	T11 CγH (w)
	NH	I18 CδH (w)
Ser 47	NH	F45 CβH (w)
	NH	D50 CβH1 (w); CβH2 (w)
	CβH	E49 NH (w)

[a] NOEs were obtained from $^{1}H-^{1}H$ and $^{1}H-^{15}N$ NOESY spectra in $^{1}H_2O$ and $^{2}H_2O$. NOE intensities were calclulated using Felix software by assigning fixed intraresidue distances to intraresidue NOEs. The designators m and w correspond to Felix distances of 2.5−3.2 and 3.2−4.5 Å, respectively. In the case of a highly mobile molecule like $[14-38]_{Abu}$, these numbers do not represent actual distances (see text for discussion). All NOEs are for the most folded (f) conformation.

antiparallel β-sheet, while 23 NH makes an H-bond with the buried side-chain carbonyl of Asn 43. In $[14-38]_{Abu}$, 21 NH and 22 NH still have the slowest exchange rates, indicating that they are in the most stable part of the structure, while 23 NH exchanges much more rapidly, suggesting that interaction between 23 NH and the 43 side chain is greatly diminished. Consistent with this, weak NOEs between the

Table 3: Hydrogen Exchange Rate Constants and Protection Factors of Slowly Exchanging Amide Hydrogens in $[14-38]_{Abu}$ at pH 4.6 and 1 °C

residue	k_{obs} (min^{-1})	k_{cx} (min^{-1})[a]	k_{cx}/k_{obs}
Ile 19	1.0×10^{-3}	1.9×10^{-2}	19
Tyr 21	3.0×10^{-3}	1.2×10^{-1}	40
Phe 22	2.8×10^{-3}	8.9×10^{-2}	32
Tyr 23	8.1×10^{-3}	8.6×10^{-2}	11
Gln 31	6.0×10^{-3}	9.3×10^{-2}	16
Phe 33	5.0×10^{-3}	1.3×10^{-1}	26
Tyr 35	4.1×10^{-3}	5.6×10^{-2}	14

[a] Intrinsic rate constants at 1 °C were calculated by the method of Bai et al. (1993) using E_a of 17 kcal/mol and pD_{corr} of 5.0.

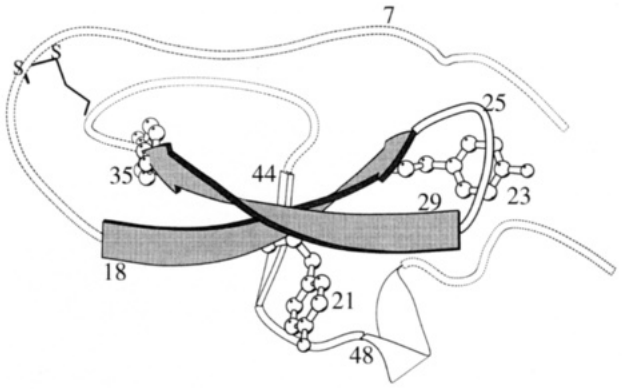

FIGURE 8: Diagram of native BPTI structure. In $[14-38]_{Abu}$, the darkened antiparallel strands of β-sheet are native-like. Also in $[14-38]_{Abu}$, residues 44−51, shown as a white ribbon drawn with solid lines, fluctuate between a major, native-like conformation and a more disordered one, while the sequences drawn with dotted lines are highly mobile and fluctuate between two or three slowly interconverting conformations. In $[14-38]_{Abu}$, the main hydrophobic contacts involve the side chains of Tyr 21, 23, and 35, shown with ball-and-stick. The figure was generated using the program MOLSCRIPT (Kraulis, 1991).

23 backbone NH and the 43 side chain NHs are observed in $[14-38]_{Abu}$ (Table 2).

Ring Conformers. In native BPTI the aromatic rings of Tyr 23, Tyr 35, and Phe 45 are conformationally restricted. Since their rings flip slowly on the NMR time scale, different chemical shifts are assigned for each of the two CδH and the two CϵH ring protons (Wagner & Wüthrich, 1982). Ring restrictions generally reflect differences in local packing environment of opposite sides of the ring. In $[14-38]_{Abu}$, two CδH (CδH1 and CδH2) and two CϵH (CϵH1 and CϵH2) peaks are assigned for the Y35 ring. While the Y35 ring is in slow exchange between two conformers, all other aromatic side chains in $[14-38]_{Abu}$ give an average signal for equivalent ring protons. The backbone protons of Y35 do not give exchange peaks.

NMR-Detected Structure of $[14-38]_{Abu}$. The essential features of $[14-38]_{Abu}$ structure at pH 4.5 and 1−10 °C are derived from the chemical shifts, exchange cross peaks, NOEs, and hydrogen isotope exchange rates (Tables 2 and 3 and Figure 7). Residues 3−7 in native BPTI are in a 3_{10}-helix (see Figure 8 for reference structure). In $[14-38]_{Abu}$ they are in equilibrium between two conformations; heteronuclear spectra (Figure 5) permit estimation of the relative populations of the conformers, 40% (f) and 60% (u). The more folded (f) has characteristics of an unstable helix. Cross peaks (f) of 3, 5, 6, and 7 have chemical shifts outside the random coil envelope and $d_{NN}(i, i+1)$ NOEs between 3 and 4 and between 5, 6, and 7 (Figure 7); however, no medium-range NOEs indicative of a stable helix are observed. The disordered conformation (u) gives random coil chemical shifts, but the presence of a strong $d_{NN}(i, i+1)$ NOE between 6 and 7 (labeled 7u/6u in Figure 5b) suggests that it is not fully extended.

Residues 10−17 in native BPTI are in an extended, aperiodic loop. In $[14-38]_{Abu}$, exchange cross peaks between (f) and (u) conformations are observed for 11, 14, and 16. The (f) conformation has chemical shifts outside the random coil envelope and has weak NOEs between T11 backbone and 35 ring atoms and between T11 side chain and 36 backbone atoms (Table 2). Lys 15 and Arg 17 NH chemical shifts (supporting information) are listed as (u) because they are closer to random coil than native. In native BPTI, this region is also quite flexible but shows additional long-range NOEs (Figure 9b).

Residues 18−35 in native BPTI compose the strand−turn−strand of the central antiparallel β-sheet containing a type I β-turn. In $[14-38]_{Abu}$, both strands are in a highly native-like conformation, while the turn is more flexible than in the native protein. Downfield chemical shifts for NH and CαH are consistent with β-sheet structures (Wishart et al., 1991). NOE evidence for a native-like antiparallel sheet includes strong $d_{\alpha N}(i, i+1)$ correlations; these are strong interstrand NH−NH NOEs between 18 and 35, 20 and 33, 22 and 31; and interstrand CαH−CαH NOEs between 19 and 34, 21 and 32, 23 and 30. Strong local tertiary contacts are indicated by NOEs between Y23 ring protons and CαH and CβH of 25 and 29−30; strong nonlocal tertiary contacts are indicated by NOEs between Y21 ring protons and the CαH and CβH of residues 46 and 48 and with 29, 30, and 32. Tertiary interactions between Ile 18 and one side of the Tyr 35 ring and between Thr 11 and Ala 40 and the other side of Tyr 35, as well as between 37 NH (f) and the 35 ring, are indicated by clear long-range NOEs (Table 2). Hydrogen isotope exchange rates of the β-sheet residues are 10−40-fold slower than in small peptides, while exchange rates of all other NHs are too fast to measure. Thus, both chemical exchange and hydrogen isotope exchange indicate that the antiparallel strands are very stable relative to the rest of the protein. Turn residues 25−28 have strong $d_{NN}(i, i+1)$ characteristic of turns, but the native-like $d_{\alpha N}(i, i+3)$ between 25 CαH and 28 NH expected for a type I β-turn (Wüthrich, 1986) is not observed. Also the presence of $d_{\alpha N}(i, i+1)$ for turn residues suggests a substantial population of flexible conformers (Dyson & Wright, 1991). The exchange peaks observed for Ala 25 likewise indicate greater flexibility of the turn in $[14-38]_{Abu}$ compared to native.

Residues 36−43 in native BPTI are in an aperiodic loop. Gly 37 NH is involved in an unusual polar network with the Tyr 35 ring and Asn 44 side chain NδH (Wlodawer et al., 1984, Tüchsen & Woodward, 1987). As a result, the 37 NH and 44 NδH have chemical shifts far upfield (3−5 ppm) and make NOEs with the Y35 ring (Tüchsen & Woodward, 1987). Also in native BPTI, Asn 43 is in an unusual location; its side chain amide is buried and donates two H-bonds to Tyr 23 O and Glu 7 O and accepts an H-bond from 23 NH. In $[14-38]_{Abu}$, residues 36−43 are much more disordered than in native BPTI. Residues 38 and 40 are in equilibrium between (f) and (u) conformations of approximately equal population (estimated from Ala 40 $^1H-^{15}N$ auto peaks). Residue 37 is especially interesting: three exchange peaks

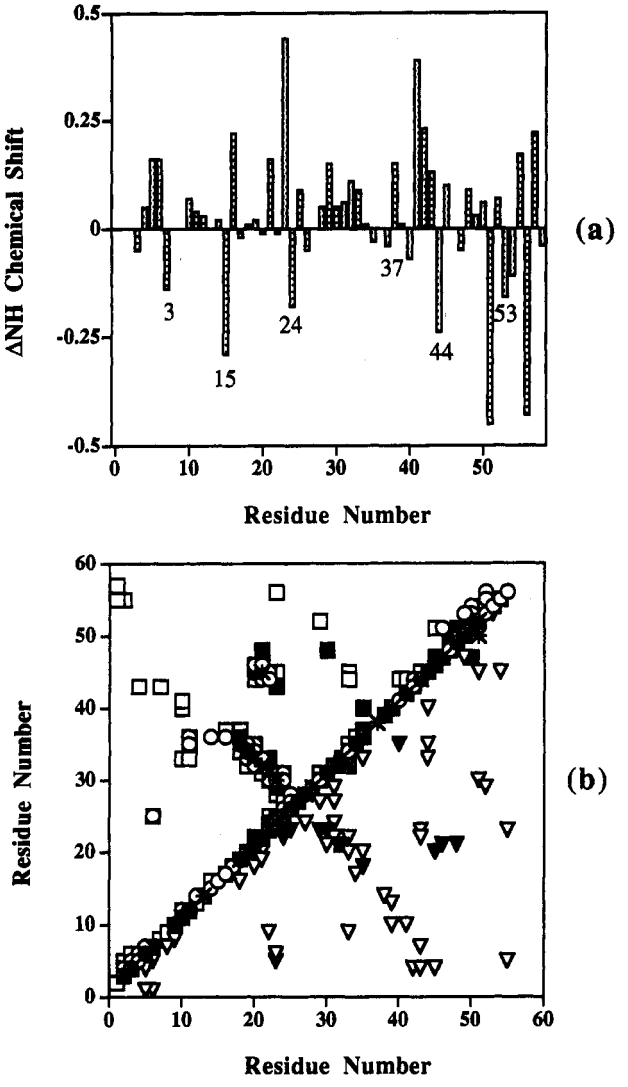

FIGURE 9: Comparison of $[14-38]_{Abu}$ with native BPTI. Panel a shows the difference in chemical shifts of the same NH in native BPTI and in the (f) conformation of $[14-38]_{Abu}$ acquired under the same conditions of temperature and pH. A downfield shift in $[14-38]_{Abu}$ corresponds to a negative difference in the plot. Panel b shows a comparison of observed NOEs between corresponding amino acid residues in native BPTI (open symbols) and in $[14-38]_{Abu}$ (filled symbols). Main-chain−main-chain NOEs (O, *) and main-chain−side-chain NOEs (□, ■) are shown above the diagonal. Side-chain−side-chain NOEs (▽, ▼) are shown below the diagonal. Most long-range NOEs in $[14-38]_{Abu}$ are from β-sheet residues to the rest of the protein. Note the reduced number of NOEs in $[14-38]_{Abu}$, reflecting more disorder.

are observed for 37 NH, indicating three slowly interconverting conformations (Figure 6). The minor (f) peak very likely reports a conformation with native-like close contact of G37 NH with the center of the Y35 ring; its unusual chemical shift (4.36 ppm) is similar to that of 37 NH in native BPTI (Tüchsen & Woodward, 1987), and it makes an NOE with the Y35 ring (Table 2). The 37 NH (u') peak has a chemical shift clearly not random coil and similar to that of 37 NH in large peptides of BPTI (Kemmink & Creighton, 1993). The third 37 NH exchange peak, (u), has the chemical shift of a fully disordered peptide. No interaction of 44 NδH with the Y35 ring is detected, and both of the 44 NδHs have chemical shifts typical of disordered peptides. Both Asn 43 and Asn 44 NδH have slower hydrogen exchange rates than model compounds. NOEs between the 35 ring and 37 CαH and between 35 CαH and 11 CαH are observed in native BPTI but not in $[14-38]_{Abu}$. Except for the Y35 ring, the only NOEs detected for residues 36−43 are $d_{NN}(i, i + 1)$ between 37 (u') and 38 (f) and between 39 (f) and 40 (f) and a weak nonlocal NOE between the 23 NH and both 43 NδHs. Note that the labeling system does not imply that all (f) cross peaks labeled report the same conformation. Rather, (f, u', u) cross peaks are defined relative to each other for the same ^1H, and each exchange cross peak is an average for rapidly interconverting conformers. Apparently the set of conformers reported by cross peak (f) for 38 NH includes those having an NOE between 38 NH (f) and 37 NH (u').

Residues 44 and 45 are in a β-bridge in native BPTI. In $[14-38]_{Abu}$ they retain the native-like β-bridge in a major conformation (f) which fluctuates with a very minor disordered conformation (u). This is illustrated by the weak exchange cross peak between 45 NH (f) at 9.95 ppm and 45 NH (u) at 8.23 ppm in TOCSY spectra. There are weak native-like long-range NOEs between 45 NH (f) and 21 NH and between 45 NH (f) and 20 CβH (Table 1). The hydrogen exchange rate of 45 NH is faster than those of other β-sheet residues but slower than random coil.

Residues 46 and 47 are in a β-bend in native BPTI and connect the short 44−45 β-bridge to the 48−56 C-terminal helix. In $[14-38]_{Abu}$, 46 and 47 retain the native-like β-bend in a major conformation (f) which is in equilibrium with a minor disordered conformation (u), as indicated by a weak exchange cross peak for 46 and 47 NHs. For (f) cross peaks, native-like sequential $d_{NN}(i, i + 1)$ NOEs are observed between 46 and 47 (Figure 7), and 47 NH has a native-like NOE to 45 CβH (Table 2). In the major (f) conformation, the β-bend interacts extensively with the first turn of the C-terminal helix (which is also intact), while the rest of the C-terminal helix is disordered. In native BPTI, Ser 47 caps the N-terminus of the 48−56 helix; the Ser 47 side chain OH forms a hydrogen bond with the Asp 50 NH, and 47 NH is within 2.8 Å of 50 CβH. Consistent with helix capping (Presta & Rose, 1988; Seale et al., 1994), medium-range NOEs are observed between Ser 47 (f) NH and Asp 50 (f) CβH2 and between Ser 47 (f) CβH and Glu 49 (f) NH. Multiple nonlocal tertiary interactions of the Tyr 21 side chain with the 46−47 bend and with 48, the first residue in the C-terminal helix, are indicated by strong NOEs between the 21 ring and CαH and CβH of Lys 46 and Ala 48. A nonlocal interaction between the central β-sheet and the first turn of the C-terminal helix is indicated by an NOE between 30 CδH and 48 CαH (Table 2).

Residues 48−56 are in an α-helix in native BPTI. In $[14-38]_{Abu}$, the major conformation of the first turn, 48−51, is native-like while the rest of the helix, 52−56, is frayed. Similar to residues 46 and 47, 48−50 NHs have exchange cross peaks indicating slow exchange between (f) and (u') conformations. For 48 NH, the (f) and (u') conformations are about equally populated (60% f, 40% u') . For (f), the sequential $d_{NN}(i, i + 1)$ NOEs for 48−52 and weak $d_{\alpha N}(i, i + 3)$ and $d_{\alpha\beta}(i, i + 3)$ between 48 and 51 (Figure 7) indicate that the first turn of the C-terminal helix is intact. For the rest of the C-terminal helix, 52−56, no NOEs indicating stable structure are observed. Furthermore, 54 and 55 NHs have (f) and (u) exchange cross peaks.

Comparison with Native BPTI. Figure 9a shows the difference in chemical shifts at 1 °C and pH 4.5 for the same NH in native BPTI and in the most folded (f) conformation

of $[14-38]_{Abu}$. Chemical shifts differ from those of native BPTI in most parts of the sequence. Chemical shifts of residues assigned to (u) and (u′) conformations deviate even more widely from native BPTI. Interresidue contacts indicated by NOEs are compared for the (f) conformation of $[14-38]_{Abu}$ and native BPTI in Figure 9b. The NOEs in native BPTI are those used by Berndt et al. (1992) in calculation of the NMR structure. While many more contacts are observed in native BPTI, those in $[14-38]_{Abu}$ are also observed in the native protein, implying that the contacts present in $[14-38]_{Abu}$ are native-like. The majority of interresidue contacts in $[14-38]_{Abu}$ involve β-sheet residues.

DISCUSSION

$[14-38]_{Abu}$ Is an Interconverting Ensemble of Partially Folded Conformations. At pH 4.5 and 1−10 °C, $[14-38]_{Abu}$ is a highly ordered β-sheet molten globule. The NMR properties of this protein indicate that it is an ensemble of partially folded conformations interconverting slowly, on the time scale of milliseconds or longer. Each conformation may have a number of conformers in rapid equilibrium. All conformations have the 18−24, 29−35 antiparallel β-sheet of native BPTI essentially intact, while in the rest of the molecule, residues undergo local order/disorder equilibria. The presence of two or three conformations, interconverting slowly enough to give rise to two or three chemical exchange peaks of the same ^{1}H, is detected for all regions of the protein except the antiparallel β-sheet. No exchange peaks are observed for residues 18−24 and 29−35, except 19 and 29, which are located at the strand ends. This implies that all conformations observed in these experiments have an intact antiparallel sheet and that resonances from fully unfolded $[14-38]_{Abu}$ do not contribute significantly to spectra. Fully unfolded conformations are, no doubt, in equilibrium with NMR-detected species, but are not sufficiently populated to be detected. Spectra also do not show the presence of fully native BPTI, further indicating that the NMR-detected species of $[14-38]_{Abu}$ under these conditions are partially folded (neither fully native nor fully unfolded).

Relative populations of interconverting conformations, and the degree of disorder indicated by chemical shifts and NOEs, vary throughout the protein; this implies that various portions of the molecule outside the antiparallel β-sheet are in local equilibria involving independent, segmental motions. Figure 8 shows the structure of native BPTI; the dark regions are those most stable in $[14-38]_{Abu}$, while the highly mobile regions are indicated by dotted lines. The regions represented by white ribbon enclosed by solid lines (residues 44−51) are more mobile than in native, but their major conformation is native-like. A broad outline of local fluctuations outside the central antiparallel β-sheet is discerned from analysis of chemical shifts, NOEs, hydrogen isotope exchange rates, and chemical exchange. The 44−45 β-bridge and the first residue of the 46−47 β-bend fluctuate between a native-like conformation (major) and a very minor more disordered conformation. The second residue of the 46−47 β-bend and the first turn (48−51) of the 48−56 C-terminal helix fluctuate between a native-like conformation (major) and a second more disordered, but not fully disordered, conformation (minor). It is clear that the 48−56 helix does not unfold as a unit; the rest of the helix (52−56) fluctuates between a fully disordered conformation and a more folded conformation which has native-like chemical shifts but is too unstable to give medium-range NOEs. Residues 3−7 (in native BPTI a 3_{10}-helix) fluctuate beween two conformations: one is highly disordered (major), and the other has characteristics of an unstable helix. The 10−17 active site loop fluctuates between two conformations: the major conformation is highly disordered; the second has native-like chemical shifts, but its only NOE is between T11 and the Y35 ring. The 36−43 loop is more disordered than in native. Gly 37 NH samples three conformations (Figure 6), a more folded (f) conformation (minor), a more disordered (u′) conformation (major) that is not a random coil, and a fully disordered (u) conformation (minor). Also in the 36−43 loop, 40 NH fluctuates between two equally populated conformations, one with NOEs to the Y35 ring and the other more disordered.

Tertiary Hydrophobic Interactions. A number of long-range NOEs indicate tertiary hydrophobic interactions in $[14-38]_{Abu}$ (Table 2). The most prominent are those of the Tyr 21 and Tyr 23 rings with turn residues and, to a smaller extent, Tyr 35 with Ile 18, Thr 11, and Ala 40. Figure 8 shows the locations of the 21, 23, and 35 rings in native BPTI. For Y23, the tertiary interactions are local, with Ala 25 (turn) and Leu 29−Abu 30 (antiparallel strand). For Y21, the tertiary interactions implied by long-range NOEs are nonlocal, the strongest being with Ala 48 (first residue of the C-terminal helix), Abu 30, and Thr 32 (antiparallel strand). Y21 also makes multiple nonlocal NOEs with Lys 46 (Table 2). The greater stabilization of the first turn (48−51) of the 48−56 helix, compared to the rest of the helix, most likely arises from interaction of Y21 with 46 and 48, along with a helix-capping hydrogen bond between the Ser 47 side chain OH and the Asp 50 NH. Ser 47 NH also has an NOE with both 45 CβHs (β-bridge).

As in native BPTI, the Y35 ring in $[14-38]_{Abu}$ shows slow chemical exchange between the two CδH protons and the two CϵH protons, implying that the ring is conformationally restricted. This is consistent with the NOEs to the Y35 ring (Table 2): 11 (f) and 40 (f) make NOEs to one side of the ring (CδH1 and CϵH1), while 18 makes NOEs to the other side (CδH2 and CϵH2). However, it is clear that the Y35 ring in $[14-38]_{Abu}$ is not packed, as it is in native BPTI. Gly 37 NH reports three conformers, and only the minor (f) conformation gives an observable NOE to the ring (Table 2). Other Y35 ring NOEs observed in native BPTI are not detected in $[14-38]_{Abu}$.

Comparison to Nonrandom Structure in Reduced BPTI. Reduced BPTI, with all three disulfides broken, lacks obvious secondary structure and is unfolded. Are there interactions in reduced BPTI that may favor formation of partially folded $[14-38]_{Abu}$? Kemmink and Creighton (1993) investigated long peptides spanning the BPTI sequence as a model of intact reduced BPTI. In these peptides, NOEs indicating six local interactions were observed. Three are observed in $[14-38]_{Abu}$ as well as in native BPTI, namely, NOEs between the 23 ring and the 25 side chain consistent with turn stabilization, between the 47 and 50 NHs consistent with helix capping, and between the 35 ring and the 37 NH consistent with a polar interaction of the 37 NH with the center of the 35 ring. Kemmink and Creighton also observed NOEs in BPTI peptides, implying a preference for three interactions *not* found in $[14-38]_{Abu}$ or native BPTI: contacts between the Y21 ring and the I19 side chain, polar interaction of the Y10 ring and G12 NH, and interactions of Y10 with

P8 and P9. The Y21/I19 interaction was also reported in BPTI peptides by Lumb and Kim (1994).

In a different type of experiment, designed to detect nonlocal interactions, Ittah and Haas (1995) report that long-range loops in reduced BPTI are stabilized by specific, nonlocal interactions which apparently do not depend on preexisting secondary structure elements. Their results indicate that a compact conformation is assumed by reduced BPTI and that a subpopulation of partially folded species has apparent native-like topology. The experiments of Ittah and Haas are particularly interesting because they are complementary to NMR; nonlocal interactions detected in fluorescence energy transfer are not necessarily expected to give NMR-detected NOEs. Consistent with the conclusion of Haas and associates that reduced BPTI has collapsed structure, reduced BPTI and $[R]_{Abu}$ (BPTI with all cysteines replaced by Abu) have clustered hydrophobes and electrophoretic mobilities similar to those of partially folded $[14-38]_{Abu}$ (Ferrer et al., 1995). Further, NMR analysis of intact, reduced BPTI and $[R]_{Abu}$ shows the presence of NOEs seen in long BPTI peptides, as well as additional hydrophobic side chain−side chain NOEs (Pan et al., 1995).

$[14-38]_{Abu}$ as a Model for Early Folding Intermediates. Early steps in the protein folding process, leading to a quasi-stable intermediate formed on the 5−20 ms time scale, are often taken as the critical events which commit the protein to its sequence-specific fold. The frequent observation that the first early intermediates are formed within 10−20 ms, but the rest of the folding process is completed on the 100 ms to 1 s time scale, is consistent with the possibility that formation of an early intermediate is a thermodynamically driven process, while later steps are kinetically determined (Matthews, 1993). We take $[14-38]_{Abu}$ to be a model for the ensemble of BPTI folding intermediates accumulated in the first 10−20 ms following formation of *any* single native disulfide bond. Consistent with this, the CD-detected secondary structure of $[14-38]_{Abu}$ is formed in $\ll$20 ms in pH jump experiments (Ferrer et al., 1995).

Taking $[14-38]_{Abu}$ as a model for early folding intermediates, the following interactions are expected to be important in initial steps in BPTI folding. The major early tertiary interactions are local *and* nonlocal hydrophobic contacts, as well as intrastrand H-bonds of the β-sheet and β-bridge. Multiple *local* hydrophobic−hydrophobic NOEs of the Y23 ring are observed with A25 (turn), L29, and Abu 30 (first residues in the strand following the turn). Multiple *nonlocal* hydrophobic−hydrophobic NOEs of the Y21 ring are observed with 46 (β-bend), 48 (first residue in C-terminal helix) and 29, 30, and 32 (strand following the 25−28 turn). Y35 NOEs are primarily nonlocal with 11 (f), 18, and 40 (f); a local NOE is observed with 37 (f). All of the local interactions on this list are consistent with NOEs in BPTI peptides and reduced BPTI (Kemmink & Creighton, 1993; Pan et al., 1995).

The observation that $[14-38]_{Abu}$ is an ensemble of partially folded species undergoing localized, segmental motion is consistent with the model of Dill and associates (Dill & Shortle, 1991) that unfolded proteins are interconverting denatured states with varying degrees of native-like structure. Local NOEs of Y23 in $[14-38]_{Abu}$ and in reduced BPTI are consistent with the idea (Dyson & Wright, 1991) that turns favored by local interactions in the unfolded protein may serve as folding initiation sites. Multiple nonlocal tertiary NOEs of the Y21 and Y35 rings support the models of Dill and associates (Dill et al., 1993; Lattman et al., 1994) in which local hydrophobic interactions (Y23−turn) that are entropically more favorable in an unfolded peptide may facilitate formation of nonlocal interactions (involving Y21 and Y35) which are entropically less favorable. The result is a cooperative "zippering" of hydrophobic interactions, which in this case occurs along with cooperative hydrogen bonds in the β-sheet. The involvement of the Y21 ring is particularly interesting. In reduced BPTI, there is a strong local interaction between Y21 and I19 side chains which would tend to keep the 19−21 region extended and therefore enhance the effectiveness of the Y23−turn interactions in initiating the antiparallel sheet. Concomitant with formation of the sheet, the 19−21 local interaction is replaced with multiple nonlocal interactions of the 21 ring with residues 29, 30, 32, 46, and 48.

$[14-38]_{Abu}$ is one of the few β-sheet molten globule structures characterized. It suggests the possibility that similar processes initiate folding of other antiparallel β-sheets, namely, local stabilization of a turn favored in the unfolded state, local stabilization in the unfolded state of an extended conformation for residues before or after that turn, and zippering of nonlocal hydrophobic contacts and sheet hydrogen bonds.

The stable sections of $[14-38]_{Abu}$ correspond to the slow-exchange core, one or more submolecular domains consisting of the elements of secondary structure carrying the cluster of 3−8 NHs with the slowest native state exchange rates, and the side chains packing these elements (Kim et al., 1993a,b; Woodward, 1993). We have proposed that the slow-exchange core is the folding core, that is, that the elements of secondary structure forming native-like structure in initial stages of folding will tend to be those of the slow-exchange core. Further, we propose that, in later stages of folding, other elements of secondary structure will tend to pack into the folded structure in reverse order of their slowest exchanging NH. One prediction of the model is that the most stable structure in equilibrium models for transient folding intermediates will tend to be the slow-exchange core. Consistent with this model, the most stable part of $[14-38]_{Abu}$ is the slow-exchange core (antiparallel β-sheet strands plus the 44−45 β-bridge), and the next most stable part is the 46−47 β-bend and the first turn of the C-terminal helix.

$[14-38]_{Abu}$ and Disulfide-Linked Folding. The organized, stable structure of $[14-38]_{Abu}$ is not in the vicinity of the 14−38 disulfide cross link, but rather in the slow-exchange core. The 10−17 and 36−43 loops containing 14 and 38 are highly flexible, as reflected in observation of multiple exchange peaks for residues 11, 14, 16, 37, 38, and 40. The primary role of the disulfide in $[14-38]_{Abu}$ is apparently to exclude more entropically stable unfolded species from accessible conformational space, thereby favoring formation of partially folded species, in all of which the most stable region is the slow-exchange core. As commonly is the case for disulfide bonds, some stabilization of partially folded species by the cystine side chain cannot be ruled out (Betz, 1993). In native BPTI, the loops containing the 14−38 disulfide retain a high degree of flexibility, as evidenced by rapid hydrogen exchange of buried NHs (Tüchsen & Woodward, 1985), ease of reduction/oxidation of the 14−38 disulfide (Goldenberg, 1988), and NMR (Otting et al., 1993).

All BPTI species with one native disulfide bond have the stable, β-sheet structure found in $[14-38]_{Abu}$. One-disulfide variants of BPTI have been studied by NMR by P. Kim and associates (Staley & Kim, 1992; 1994; Schulman & Kim, 1994), where Cys is replaced by Ala, and by Creighton and associates (van Mierlo et al., 1991, 1993), where Cys is replaced by Ser. Whereas in $[14-38]_{Abu}$ with the cross link between flexible loops, the core β-sheet is formed, in $[30-51]_{Ser}$ and $[30-51]_{Ala}$ with the cross link between the sheet and C-terminal helix, the core plus the C-terminal helix is formed, while in $[5-55]_{Ser}$ and $[5-55]_{Ala}$ with the cross link between the C- and N-terminal helices, the core plus both the C- and N-terminal helices are formed. Hydrogen exchange patterns in $[5-55]_{Ala}$ (Schulman & Kim, 1994) indicate that many NHs exchange by the unfolding mechanism (Woodward et al., 1982; Kim & Woodward, 1993), which prevents measurement of the slow-exchange core of this protein. Relative stabilities of one-disulfide species are difficult to assess since cysteines are variously replaced with Ala, Ser, or Abu. We chose α-amino-*n*-butyric acid because it has the same number of heavy atoms and the same charge as cysteine in the thiol form, which at physiological pH is the primary species of cysteine in reduced BPTI. $[14-38]_{Abu}$ has a cooperative folding/unfolding transition with a T_m of 19 °C (Ferrer et al., 1995). $[5-55]_{Ser}$ and $[5-55]_{Ala}$ have T_m values of <15 and ~40 °C, respectively. $[30-51]_{Ser}$ unfolds at ≥15 °C, and $[30-51]_{Ala}$, at 35 °C.

The dynamic structure of $[14-38]_{Abu}$ gives insight into early species formed in *any* sequence of disulfide bond formation and does not depend on questions and controversies concerning the later maturation of disulfide bond arrangements. We propose that formation of *any* native disulfide bond decreases the chain entropy of extended species, and thereby leads to rapid, cooperative formation of an interconverting ensemble in which the slow-exchange core is more stable, while the rest of the molecule is more mobile. If the disulfide involves residues in one helix (30–51), that helix is stabilized relative to its more flexible conformations in $[14-38]_{Abu}$. Similarly, if the disulfide involves residues in two helices (5–55), both helices are stabilized relative to their more flexible conformations in $[14-38]_{Abu}$. Subsequent formation or rearrangement of disulfide bonds favors formation of helices by destabilizing more flexible conformations of helical segments, by consolidation of buried side chains of disulfides 5–55 and 30–51 in a hydrophobic cluster, and perhaps by other native-state effects. In native BPTI, only the side chains of 5–55 and 30–51 have the packing environment (Bowie et al., 1991) of a hydrophobic cluster [Table 3 in Kim et al. (1993a)]; other hydrophobic side chains are packed in a much more polar local environment.

ADDED IN PROOF

In a recent reexamination of disulfide-linked folding of BPTI, Dadlez and Kim (1995) have detected the presence of the 14–38 single-disulfide species and proposed that it is an important early kinetic intermediate.

SUPPORTING INFORMATION AVAILABLE

A table of backbone and side chain assignments of $[14-38]_{Abu}$ (3 pages). Ordering information is given on any current masthead page.

REFERENCES

Alexandrescu, A. T., Evans, P. A., Pitkeathly, M., Baum, J., & Dobson, C. M. (1993) *Biochemistry 32,* 1707–1718.

Bai, Y., Milne, J. S., Mayne, L., & Englander, S. W. (1993) *Proteins 17,* 75–86.

Baldwin, R. (1993) *Curr. Opin. Struct. Biol. 2,* 6–12.

Baum, J., Dobson, C. M., Evans, P. A., & Hanley, C. (1989) *Biochemistry 28,* 7–13.

Bax, A., & Davis, D. G. (1985) *J. Magn. Reson. 63,* 207–213.

Bax, A., Griffey, R. H., & Hawkins, B. L. (1983) *J. Magn. Reson. 55,* 301–315.

Berndt, K. D., Güntert, P., Orbons, L. P. M., & Wüthrich, K. (1992) *J. Mol. Biol. 227,* 757–775.

Betz, S. (1993) *Protein Sci. 2,* 1551–1558.

Bodenhausen, G., & Ruben, D. (1980) *Chem. Phys. Lett. 69,* 185–189.

Bothner-By, A., Stephens, R., Lee, J., Warren, C., & Jeanloz, R. (1984) *J. Am. Chem. Soc. 106,* 811–813.

Bowie, J. U., Lüthy, R., & Eisenberg, D. (1991) *Science 253,* 164–170.

Dadle, M., & Kim, P. (1995) *Nature, Struct. Biol. 2,* 674–679.

Dill, K., & Shortle, D. (1991) *Annu. Rev. Biochem. 60,* 795–825.

Dill, K., Fiebig, K., & Chan, H. (1993) *Proc. Natl. Acad. Sci. U.S.A. 90,* 1942–1946.

Dobson, C. (1992) *Curr. Opin. Struct. Biol. 2,* 6–12.

Driscoll, P. C., Gronenborn, A. M., Wingfield, P. T., & Clore, G. M. (1990) *Biochemistry 29,* 4668–4682.

Dyson, J., & Wright, P. (1991). *Annu. Rev. Biochem. 60,* 795–825.

Farrow, N. A., Zhang, O., Forman-Kay, J. D., & Kay, L. E. (1994) *J. Biomol. NMR 4,* 727–734.

Farrow, N. A., Zhang, O., Forman-Kay, J. D., & Kay, L. E. (1995) *Biochemistry 34,* 868–878.

Ferrer, M., Woodward, C., & Barany, G. (1992) *Int. J. Pept. Protein Res. 40,* 194–207.

Ferrer, M., Barany, G., & Woodward, C. (1995) *Nature Struct. Biol. 2,* 211–218.

Goldenberg, D. P. (1988) *Biochemistry 27,* 2481–2489.

Griesinger, C., Otting, K., Wüthrich, K., & Ernst, R. R. (1988) *J. Am. Chem. Soc. 110,* 7870–7872.

Hore, P. J. (1983) *J. Magn. Reson. 55,* 283–300.

Hughson, F. M., Wright, P. E., & Baldwin, R. L. (1990) *Science 249,* 1544–1548.

Ittah, V., & Haas, E. (1995) *Biochemistry 34,* 4493–4506.

Jeener, J., Meier, B. H., Bachmann, P., & Ernst, R. R. (1979) *J. Chem. Phys. 71,* 4546–4553.

Jeng, M. F., & Englander, S. W. (1991) *J. Mol. Biol. 221,* 1045–1061.

Jennings, P., & Wright, P. (1993) *Science 262,* 892–896.

Kemmink, J., & Creighton, T. (1993) *J. Mol. Biol. 234,* 861–878.

Kim, K.-S., & Woodward, C. (1993) *Biochemistry 32,* 9609–9613.

Kim, K.-S., Fuchs, F., & Woodward, C. (1993a) *Biochemistry 32,* 9600–9608.

Kim, K.-S., Tao, F., Fuchs, J., Danishefsky, A., Housset, D., Wlodawer, A., & Woodward, C. (1993b) *Protein Sci. 2,* 588–596.

Kraulis, P. J. (1991) *J. Appl. Crystallogr. 24,* 946–950.

Lattman, E., Fiebig, K., & Dill, K. (1994) *Biochemistry 33,* 6158-6166.

Lumb, K., & Kim, P. (1994) *J. Mol. Biol. 236,* 412–420.

Marion, D., & Wüthrich, K. (1983) *Biochem. Biophys. Res. Commun. 113,* 967–974.

Matthews, C. R. (1993) *Annu. Rev. Biochem. 62,* 653–683.

Messerle, B. A., Wider, G., Otting, G., Weber, C., & Wüthrich, K. (1989) *J. Magn. Reson. 85,* 608–613.

Neri, D., Billeter, M., Wider, G., & Wüthrich, K. (1992) *Science 257,* 1559–1563.

Otting, G., Liepinsh, E., & Wüthrich, K. (1993) *Biochemistry 32,* 3571–3582.

Pan, H., Barbar, E., Barany, G., & Woodward, C. (1995) *Biochemistry* (in press).

Piotto, M., Saudek, V., & Sklenar, V. (1992) *J. Biomol. NMR 2,* 661–665.

Presta, L. G., & Rose, G. D. (1988) *Science 240*, 1632−1641.
Ptitsyn, O. (1992) in *Protein Folding* (Creighton, T., Ed.) pp 243−300, W. H. Freeman & Co., New York.
Redfield, C., Smith, A., and Dobson, C. (1994) *Nature Struct. Biol. 1*, 23−29.
Sandström, J. (1982) *Dynamic NMR*, Academic Press, New York.
Schulman, B., & Kim, P. (1994) *Protein Sci. 3*, 2226−2232.
Seale, J. W., Srinivasan, R., & Rose, G. (1994) *Protein Sci. 3*, 1741−1745.
Shaka, A. J., Keeler, J., Frenkiel, T., & Freeman, R. (1983) *J. Magn. Reson. 52*, 335−338.
Staley, J., & Kim, P. (1992) *Proc. Natl. Acad. Sci. U.S.A. 89*, 1519−1523.
Staley, J. P., & Kim, P. S. (1994) *Protein Sci. 3*, 1822−1832.
Tüchsen, E., & Woodward, C. (1985) *J. Mol. Biol. 185*, 405−419.
Tüchsen, E., & Woodward, C. (1987) *Biochemistry 26*, 1918−1925.
van Mierlo, C., Darby, N., Neuhaus, D., & Creighton, T. (1991) *J. Mol. Biol. 222*, 373−390.
van Mierlo, C., Darby, N., Keeler, J., Neuhaus, D., & Creighton, T. (1993) *J. Mol. Biol. 229*, 1125−1146.
Wagner, G., & Wüthrich, K. (1982) *J. Mol. Biol. 155*, 347−366.
Wagner, G., Braun, W., Havel, T. F., Schaumann, T., Gò, N., & Wüthrich, K. (1987) *J. Mol. Biol. 196*, 611−639.
Wishart, D. S., Sykes, B. D., & Richards, F. M. (1991) *J. Mol. Biol. 222*, 311−333.
Wlodawer, A., Walter, J., Huber, R., & Sjölin, L. (1984) *J. Mol. Biol. 180*, 301−329.
Woodward, C. (1993) *Trends Biochem. Sci. 18*, 359−360.
Woodward, C., Simon, I., & Tüchsen, E. (1982) *Mol. Cell. Biochem. 48*, 135−160.
Wüthrich, K. (1986) *NMR of Proteins and Nucleic Acids,* Wiley and Sons, New York.
Zhang, O. W., Kay, L. E., Olivier, J. P., & Forman-Kay, J. D. (1994) *J. Biomol. NMR 4*, 845−858.

BI951022E